WAVE-INDUCED CURRENT FOR LONG-CRESTED AND SHORT-CRESTED RANDOM WAVES

Dag Myrhaug[1] and Lars Erik Holmedal
Department of Marine Technology
Norwegian University of Science and Technology
NO-7491 Trondheim, Norway
[1]E-mail: dag.myrhaug@ntnu.no
Phone: +47 73 59 55 27
Fax: +47 73 59 55 28

Abstract

This paper provides a simple analytical tool which can be used to calculate the wave-induced current beneath long-crested (2D) and short-crested (3D) random waves. The approach is based on assuming the waves to be a stationary narrow-band random process and by adopting the Forristall (2000) wave crest height distribution representing both 2D and 3D Stokes second order random waves. An example is included to illustrate the applicability of the results for practical purposes using data typical for field conditions; the significant values of the Stokes drift and transport in deep water and in finite water depth are calculated. The present analytical results can be used to make assessment of the wave-induced current based on available wave statistics.

Keywords: Surface gravity waves; Stokes drift; Long-crested waves; Short-crested waves; Stokes second order random waves; Stochastic method.

1. Introduction

The Stokes drift represents an important transport mechanism in the ocean, which locally are responsible for material tracer evolution (e.g. plankton, larvae, contaminated ballast water from ships, oil spills). It is also involved in air-sea mixing processes across the interphase between the atmosphere and the ocean. The Stokes drift is obtained as the mean Lagrangian velocity giving the water particle drift in the wave propagation direction. This drift has its maximum at the surface and decreases towards the bottom. The total mean mass transport is obtained as the integral over the water depth of the Stokes drift; this is also referred to as the volume Stokes transport by Rascle et al. (2008). More details of the Stokes drift are given in e.g. Dean and Dalrymple (1984).

The Stokes drift and the volume Stokes transport are commonly defined for regular waves. However, their characteristic quantities are also defined for random waves in terms of the sea state parameters significant wave height and characteristic wave periods (e.g Rascle et al. (2008); Webb and Fox-Kemper (2011). Rascle et al. (2008) described a global data base for parameters associated with ocean surface mixing and drift, which included the surface Stokes drift and the volume Stokes transport among other parameters by performing wave hindcast of the wave parameters. Rascle and Ardhuin (2013) improved the hindcast results of Rascle et al. (2008) by using new parameterizations of the physical processes involved (more details are given in the references therein). Webb and Fox-Kemper (2011) considered relationships between the wave spectral moments and the Stokes drift in deep water at an arbitrary elevation in the water column, and intercomparisons were made using different spectral formulations. Myrhaug (2013, in press) presented bivariate distributions of significant wave height with surface Stokes drift and volume Stokes transport. Myrhaug (2013) also

presented bivariate distributions of spectral peak period with these two Stokes drift parameters together with example of results corresponding to typical field conditions.

The purpose of this study is to provide a simple analytical tool which can be used to give estimates of the significant value of the wave-induced current, i.e. the Stokes drift as well as the Stokes transport, within a sea state of long-crested (2D) and short-crested (3D) Stokes second order random waves. The approach is based on assuming the waves to be a stationary narrow-band random process and adopting the Forristall (2000) wave crest height distribution representing both 2D and 3D random waves. The cumulative distribution function of Stokes drift and Stokes transport for individual random waves are determined, from which the statistical properties of both quantities can be calculated. Thus this approach is more mathematically sound than by using characteristic statistical values of the waves in the regular wave formulas. An example is also included to illustrate the applicability of the results for practical purposes using data typical for field conditions.

2. Background for regular waves

Following Dean and Dalrymple (1984) the mean (time-averaged) Lagrangian mass transport at an elevation z_1 in the water column in finite water depth h is given as

$$\bar{u}_L = \frac{ga^2k^2}{\omega}\frac{\cosh 2k(z_1+h)}{\sinh 2kh} \tag{1}$$

Here, g is the acceleration due to gravity, a is the linear wave amplitude, k is the wave number corresponding to the cyclic wave frequency ω given by the dispersion relationship $\omega^2 = gk\tanh kh$. Eq. (1) indicates that the water particles drift in the wave propagation direction; this drift has its maximum at the mean free surface $z_1 = 0$ and decreases towards the bottom as $z_1 \to -h$. In deep water Eq. (1) reduces to

$$\bar{u}_L = \frac{ga^2k^2}{\omega} e^{2kz_1} \quad ; \quad \omega^2 = gk \tag{2}$$

The Langrangian mass transport is often referred to as Stokes drift.

The total mean (time- and depth-averaged) mass transport is given as (Dean and Dalrymple, 1984)

$$M = \frac{\rho g a^2 k}{2\omega} \tag{3}$$

where ρ is the density of the fluid. M is often referred to as the Stokes transport. More details of the Stokes drift and the Stokes transport are given in Dean and Dalrymple (1984).

3. Present analytical calculation of wave-induced drift in random waves

At a fixed point in a sea state with stationary narrow-band random waves consistent with Stokes second order regular waves in finite water depth, the non-dimensional nonlinear crest height, $w_c = \eta_c / a_{rms}$ is

$$w_c = \hat{a} + O(k_p a_{rms}) \tag{4}$$

Here $\hat{a} = a / a_{rms}$ is the non-dimensional linear wave amplitude, where the linear wave amplitude a is made dimensionless with the root-mean-square (*rms*) value a_{rms}. Moreover, $O(k_p a_{rms})$ denotes the second order (nonlinear) terms, which are proportional to the characteristic wave steepness of the sea state, $k_p a_{rms}$, where k_p is the wave number corresponding to ω_p (=peak frequency of the wave spectrum) given by the dispersion relationship for linear waves (which is also valid for the Stokes second order waves)

$$\omega_p^2 = g k_p \tanh k_p h \tag{5}$$

Now Eq. (4) can be inverted to give $\hat{a} = w_c - O(k_p a_{rms})$. By substituting this in Eq. (1), the non-dimensional Stokes drift for individual random waves, $u = \bar{u}_L / u_{Lrms}$, is given as

$$u = w_c^2 \tag{6}$$

where

$$u_{Lrms} = \frac{g a_{rms}^2 k_p^2}{\omega_p} \frac{\cosh 2k_p(z_1 + h)}{\sinh 2k_p h} \tag{7}$$

In deep water Eq. (7) reduces to

$$u_{Lrms} = \frac{g a_{rms}^2 k_p^2}{\omega_p} e^{2k_p z_1} \quad ; \quad \omega_p^2 = g k_p \tag{8}$$

Similarly, the non-dimensional Stokes transport for individual random waves, $m = M / M_{rms}$, is given as

$$m = w_c^2 \tag{9}$$

where

$$M_{rms} = \frac{\rho g a_{rms}^2 k_p}{2\omega_p} \tag{10}$$

It should be noted that strictly speaking, the non-dimensional Stokes drift (and the non-dimensional Stokes transport) is related to both wave crest height and wave number. For example, in deep water, $\omega^2 = gk$ and $\omega_p^2 = gk_p$, and consequently the non-dimensional Stokes transport is given by

$$m = M/M_{rms} = \left(\frac{\rho g a^2 k}{2\omega}\right) \Big/ \left(\frac{\rho g a_{rms}^2 k_p}{2\omega_p}\right) = \frac{a^2}{a_{rms}^2} \sqrt{\frac{k}{k_p}} = w_c^2 \sqrt{\frac{k}{k_p}}.$$

However, under the assumption of narrow-band wave spectrum (i.e. $k = k_p$), the relations suggested in this paper are acceptable approximations.

Now the Forristall (2000) parametric crest height distribution based on simulations using second order theory is adopted. The simulations were based on the Sharma and Dean (1981) theory; this model includes both sum-frequency and difference-frequency effects. The simulations were made both for 2D and 3D random waves. A two-parameter Weibull distribution with the cumulative distribution function (*cdf*) of the form

$$P(w_c) = 1 - \exp\left[-\left(\frac{w_c}{\sqrt{8}\alpha}\right)^{\beta}\right]; \quad w_c \geq 0 \tag{11}$$

was fitted to the simulated wave data. The Weibull parameters α and β were estimated from the fit to the simulated wave data, and are based on the wave steepness S_1 and the Ursell parameter U_R defined by

$$S_1 = \frac{2\pi H_s}{g T_1^2} \tag{12}$$

and

$$U_R = \frac{H_s}{k_1^2 h^3} \tag{13}$$

Here H_s is the significant wave height, T_1 is the spectral mean wave period and k_1 is the wave number corresponding to T_1. The wave steepness and the Ursell number characterize the degree of nonlinearity of the waves in finite water depth. At zero steepness and zero Ursell number fits were forced to match the Rayleigh distribution, i.e. $\alpha = 1/\sqrt{8} \approx 0.3536$ and $\beta = 2$. Note that this is the case for both 2D and 3D linear waves. The resulting parameters for the 2D-model are

$$\begin{aligned} \alpha_{2D} &= 0.3536 + 0.2892 S_1 + 0.1060 U_R \\ \beta_{2D} &= 2 - 2.1597 S_1 + 0.0968 U_R^2 \end{aligned} \tag{14}$$

and for the 3D-model

$$\begin{aligned} \alpha_{3D} &= 0.3536 + 0.2568 S_1 + 0.0800 U_R \\ \beta_{3D} &= 2 - 1.7912 S_1 - 0.5302 U_R + 0.284 U_R^2 \end{aligned} \tag{15}$$

Forristall (2000) demonstrated that the wave set-down effects were smaller for short-crested than for long-crested waves, which is due to that the second-order negative difference-frequency terms are smaller for 3D waves than for 2D waves. Consequently the wave crest heights are larger for 3D waves than for 2D waves.

The sum-frequency and difference frequency effects arise from adding together all the frequency components which give second order terms with frequencies equal to the sum of two pair frequencies (sum-frequencies), and second order terms with frequencies equal to the difference of two pair frequencies (difference-frequencies). The terms with the sum-frequencies represent the short period second wave order components, while those with the difference-frequencies represent the long period second order wave components. The second order effects increase with decreasing water depth. The difference frequency terms have almost no effect in deep water (for a narrow-band process it is zero). But as the water depth decreases, these terms become more significant, and are almost of the same magnitude as the sum-frequency terms. The sum-frequency terms are positive giving a wave set-up, while the difference-frequency terms are negative giving a reduction of the second order component leading to a wave set-down. More discussion of the differences between 2D and 3D second order waves will be given in Sections 4.1 and 4.2 for deep water and finite water depth, respectively.

It should be noted that based on the narrow-band assumption $H_s = \sqrt{2}H_{rms} = 2\sqrt{2}a_{rms}$ and $T_p = T_1$.

Based on the Forristall distribution the *cdf* of u (and m) is obtained by transformation of random variables, i.e. by using Eqs. (6) and (9) it follows that the *cdf* of u (and m) is given by the two-parameter Weibull *cdf* of the form

$$P(x) = 1 - \exp\left[-\left(\frac{x}{\hat{\alpha}}\right)^{\hat{\beta}}\right] \quad ; \quad x \geq 0 \tag{16}$$

where x represents u and m, and the Weibull parameters are given as

$$\hat{\alpha} = (\sqrt{8}\alpha)^2 \quad ; \quad \hat{\beta} = \frac{\beta}{2} \tag{17}$$

It should be noted that Forristall (2000) presented the results in a wide parameter range; $0<S_1<0.15$ and $0<U_R<1$. The values of S_1 and U_R typical of the real sea state conditions given in the example of applications in Section 5, are in these ranges.

The results for linear waves referred to here are given by the *cdf* in Eqs. (16) and (17) for $\alpha=1/\sqrt{8}$, $\beta=2$ giving $\hat{\alpha}=1,\hat{\beta}=1$, i.e. corresponding to the exponential *cdf*. For the other values of $\hat{\alpha}$ and $\hat{\beta}$ the results are referred to as nonlinear, i.e. corresponding to the results based on a Weibull *cdf*.

A statistical quantity of interest is the expected value of the $(1/n)$th largest values of the wave-induced current, i.e.

$$E[x\,|\,x>x_{1/n}]=n\int_{x_{1/n}}^{\infty}xp(x)dx \tag{18}$$

where $p(x)=dP(x)/dx$ with $P(x)$ as given in Eq. (16) is the probability density function (*pdf*) of x, and $x_{1/n}$ is the value of x which is exceeded by the probability $1/n$, i.e. determined from $1-P(x_{1/n})=1/n$ as $x_{1/n}=\hat{\alpha}(\ln n)^{1/\hat{\beta}}$. By using this, the result of Eq. (18) is

$$E[x\,|\,x>x_{1/n}]=n\hat{\alpha}\,\Gamma(1+\frac{1}{\hat{\beta}},\ln n) \tag{19}$$

where $\Gamma(\bullet,\bullet)$ is the incomplete gamma function (see e.g. Abramowitz and Stegun (1972, Ch. 6.5, Eq. (6.5.3))).

For linear waves $(\hat{\alpha}=1,\hat{\beta}=1)$, Eq. (19) reduces to

$$E[x\,|\,x>x_{1/n}]=n\Gamma(2,\ln n) \tag{20}$$

4. Results and discussion

A feature of interest is to compare the nonlinear results with the corresponding linear results for both 2D and 3D waves (i.e. for $\hat{\alpha}=1,\hat{\beta}=1$). Here this will be illustrated by

considering the significant value (i.e. n = 3). However the most appropriate statistical value to use will depend on the problem considered. The nonlinear – to – linear ratio of the significant value of the Stokes drift (and the Stokes transport) based on Eqs. (19) and (20) is obtained as

$$R_1 = \frac{n\hat{\alpha}\,\Gamma(1+\frac{1}{\hat{\beta}}, \ln n)}{n\Gamma(2, \ln n)} = \frac{8\alpha^2\,\Gamma(1+\frac{2}{\beta}, \ln n)}{\Gamma(2, \ln n)} \tag{21}$$

Another interesting feature is to compare the 3D and 2D results. The ratio of the significant value ($n=3$) of the Stokes drift (and Stokes transport), for 3D waves to the significant value ($n=3$) of the Stokes drift (and Stokes transport) for 2D waves based on Eq. (19) is obtained as

$$R_2 = \left(\frac{\alpha_{3D}}{\alpha_{2D}}\right)^2 \frac{\Gamma(1+\frac{2}{\beta_{3D}}, \ln n)}{\Gamma(1+\frac{2}{\beta_{2D}}, \ln n)} \tag{22}$$

It should be noted that R_1 and R_2 depend on S_1 and U_R via the Weibull parameters α and β (Eqs. (14) and (15)).

4.1 Deep water

Here the results for deep water are considered. Now $U_R = 0$ and thus the results only depend on S_1. As referred to in Section 3, the second order negative difference-frequency effects disappear in deep water; only the second order sum-frequency effects are present, and consequently there are no wave set-down effects in deep water. Moreover, the sum-frequency effects are larger for 2D waves than for 3D waves in deep water, yielding higher wave crests for 2D waves than for 3D waves. Thus this yields larger wave-induced velocities beneath the wave crests for 2D waves than for 3D waves. The consequences of these features for the Stokes drift (and the Stokes transport) in deep water are demonstrated in Figs. 1 and 2.

Figure 1 shows the nonlinear – to – linear ratio R_1 for 2D and 3D waves in deep water versus the wave steepness S_1. For both 2D and 3D waves it appears that R_1 increases as S_1 increases, which is physically sound. These features are also demonstrated in Fig. 2, which shows the ratio R_2 of the 3D - to - 2D results versus S_1. It appears that the significant value of the Stokes drift (and the Stokes transport) is always smaller for 3D waves than for 2D waves; it is in the range 94 to 95 per cent for $S_1 = 0.15$. This behavior is caused by the smaller sum-frequency effect for 3D waves than for 2D waves in deep water.

4.2 Finite water depth

Now the results for finite water depths are considered. As referred to in Section 3, both second order sum-frequency and second order difference-frequency effects are present in finite water depths. The second order negative difference-frequency effects are smaller for 3D waves than for 2D waves, leading to smaller wave set-down effects for 3D waves than for 2D waves. This is the dominating effect for finite water depths, yielding higher wave crests for 3D waves than for 2D waves, i.e. contrary to the deep water case. Thus this yields larger wave-induced velocities beneath the wave-crests for 3D waves than for 2D waves. The consequences of these features for the Stokes drift (and the Stokes transport) in a finite water depth are demonstrated in Figs. 3, 4 and 5.

Figures 3 and 4 show the isocurves for the nonlinear – to – linear ratio R_1 for 2D and 3D waves, respectively, versus the wave steepness S_1 and the Ursell number U_R. Overall, Figs. 3 and 4 exhibit the same features; for both 2D and 3D waves it appears that, for a given value of U_R, i.e. at a given water depth, R_1 increases as S_1 increases and, for a given value of S_1, R_1 increases as U_R increases (i.e. as the water depth decreases). These features are physically sound. For the significant value of the wave-induced current, R_1 ranges up to about

2.2 for 2D waves (Fig. 3) and up to about 2.4 for 3D waves (Fig. 4). Thus it appears that R_1 is slightly larger for 3D waves than for 2D waves except for smaller values of U_R. These features are demonstrated in Fig. 5 which shows isocurves for the ratio R_2 of the 3D - to - 2D results versus S_1 and U_R. Except for the smaller values of U_R (i.e. for U_R smaller than about 0.2), it appears that the significant value of the wave-induced current is always slightly larger for 3D waves than for 2D waves. Overall, R_2 increases as U_R increases (i.e. as the water depth becomes shallower). This behaviour is caused by the smaller wave set-down effects for short-crested waves than for long-crested waves in finite water depths. However, for a given value of $U_R \lesssim 0.4$, i.e. corresponding to relative deep water, it appears that R_2 decreases as S_1 increases. This is due to the smaller negative wave set-down effects for both 2D and 3D waves, while the positive wave setup effect is larger for 2D than for 3D waves. Consequently the wave-induced current is larger for 2D than for 3D waves. For a given value of $U_R \gtrsim 0.7$, i.e. corresponding to relative shallow water, it appears that R_2 increases as S_1 increases. This is due to the smaller wave set-down effect for 3D than for 2D waves, and consequently the wave-induced current is larger for 3D than for 2D waves. However, the difference in the results for 2D and 3D waves are small, i.e. R_2 is in the range 0.95 to 1.06. The reason for the shape of the R_2-isocurves of 1.05 and 1.06 is not known; it might arise from the parameterization upon which the Forristall (2000) distribution is based. It should be noted that the results for $U_R = 0$ in Figs. 3, 4 and 5 are the same as those presented in Figs. 1 and 2.

5. Example of results

To the authors' knowledge no data on Stokes drift due to nonlinear random waves are available in the open literature. Hence two examples are included to illustrate the applicability

of the results for practical purposes using data typical for field conditions, corresponding to deep water and finite water depth flow conditions, respectively.

Table 1 gives the flow conditions and the results in terms of the significant drift corresponding to the results in Figs. 1 to 5. For the Stokes drift the results are exemplified by calculating the surface Stokes drift, i.e. by taking $\bar{u}_L = u_{Lrms}$ where u_{Lrms} is evaluated at $z_1 = 0$; $u_{Lrms} = g a_{rms}^2 k_p^2 / \omega_p$ and $k_p = \omega_p^2 / g$.

In deep water it appears that the significant value of the surface wave-induced current $(\bar{u}_L)$ for linear waves, 2D and 3D waves are 0.0881 m/s, 0.0950 m/s and 0.0940 m/s, respectively. The corresponding values of the Stokes transport (M/ρ) are 0.491 m^2/s, 0.529 m^2/s and 0.524 m^2/s, respectively.

In finite water depth $(h = 15\,m)$ the corresponding values of $\bar{u}_L$ are 0.108 m/s, 0.121 m/s, 0.119 m/s, and the corresponding values of M/ρ are 0.546 m^2/s, 0.609 m^2/s, 0.597 m^2/s.

It should be noted that for these values of S_1 and U_R, the wave-induced current for 3D waves is slightly smaller than that for 2D waves, which is consistent with the results in Fig. 5.

A frequently asked question is: What is the ratio between the wave-induced current and the mean wind speed at the 10 m elevation above the sea surface (U_{10})?

This issue is considered here by choosing a Phillips spectrum as the deep water wave spectrum (see e.g. Tucker and Pitt (2001)).

$$S(\omega) = \alpha \frac{g^2}{\omega^5} \quad ; \quad \omega \geq \omega_p = \frac{g}{U_{10}} \tag{23}$$

where $\alpha = 0.0081$ is the Phillips constant. By using the definition of the zeroth spectral moment

$$m_0 = \int_0^\infty S(\omega) d\omega \tag{24}$$

it follows that

$$H_s = 4\sqrt{m_0} = \frac{2\sqrt{\alpha}}{g} U_{10}^2 \tag{25}$$

Moreover,

$$T_p = \frac{2\pi}{\omega_p} = \frac{2\pi}{g} U_{10} \tag{26}$$

According to this it follows that the given values of $H_s = 2\,\text{m}$ and $T_p = 6.7\,\text{s}$ corresponds to $U_{10} = 10.4\,\text{m/s}$.

Based on the results in Table 1 it appears that the ratio between the significant value of the surface Stokes drift in deep water and the mean wind speed at the 10 m elevation $(\overline{u}_L / U_{10})$ is about 0.9%. This is consistent with the results obtained by Rascle et al. (2008), who described a global data base for parameters associated with ocean surface mixing and drift including the surface Stokes drift in deep water. For a wind speed of $U_{10} = 10.4\,\text{m/s}$ they obtained surface Stokes drift values in the range 0.8% to 1.6% of U_{10} in the open ocean; (see Rascle et al. (2008, Fig. 8)).

For directional seas the reduction compared with the 2D results are about 20% (Rascle and Ardhuin (2013)). It should be noted that a very similar reduction in the surface Stokes drift was also suggested in Webb and Fox-Kemper (2011; Appendix 4). Moreover, the effects of directional spreading and multidirectional waves have been further explored by Webb (2013; Ch. 2), suggesting that more interesting effects occur when swell and wind waves coexist with different directional properties. Both in the present example and in Fig. 2 it appears that the reduction of the 3D results compared with the 2D results are smaller than the 20% reduction obtained by Rascle and Ardhuin (2013). This smaller reduction of about 6% (Fig. 2) is mainly due to the inherent properties of the Forristall (2000) wave crest height distribution containing the relatively weak Stokes second order nonlinear effects.

Based on the results in Table 1 it also appears that the surface Stokes drift in a finite water depth is about 1.2% of U_{10}. Moreover, it appears that the Stokes transport (M/ρ) is about 5% and 6% of U_{10} in deep and finite water depth, respectively.

It should be noted that a commonly used procedure of estimating the significant values of the Stokes drift for random waves would be to use Eqs. (1) to (3) and substitute for H_s and T_p, i.e. to substitute $a = H_s/2 = \sqrt{2}a_{rms}$, $k=k_p$ and $\omega = \omega_p = 2\pi/T_p$. By referring to this as the deterministic method, the results are that $\bar{u}_{L\det} = 2u_{Lrms}$ where u_{Lrms} is given in Eqs. (7) and (8) for finite and deep water, respectively; and $M_{\det} = 2M_{rms}$ where M_{rms} is given in Eq. (10). These values are also given in Table 1 for finite and deep water. Thus, for linear waves in this example, it appears that the ratio between the stochastic and the deterministic method is 1.05 both for $\bar{u}_L$ and M. Moreover, the surface Stokes drift is about 0.8% of U_{10}=10.4 m/s, which is in the range of 0.8% -1.6% as reported by Rascle et al. (2008). However, it should be noted that the effects of wave nonlinearity due to 2D and 3D Stokes second order waves are not possible to estimate by using the deterministic method. Hence this stochastic approach is more mathematically sound than by using the significant wave height and the spectral peak period in an otherwise deterministic method. Moreover, it also provides results which arises from 2D and 3D Stokes second order wave nonlinearities inherent in the Forristall (2000) parametric wave crest height distribution. However, comparison with data are required before a conclusion regarding the validity of the approach can be given. In the meantime the approach should be of practical interest for estimating Stokes drift based on available wave statistics.

6. Summary and conclusions

A simple analytical tool which can be used to give estimates of statistical values of the wave-induced current beneath long-crested (2D) and short-crested (3D) nonlinear random waves is provided. The statistical values of the wave-induced current considered here are the significant values of the Stokes drift and the Stokes transport. The present analytical results can be used to make assessment of the wave-induced current based on available wave statistics.

The main conclusions can be summarized as follows:

1) In deep water, for both 2D and 3D nonlinear waves, the wave-induced current is larger than for linear waves, and the difference increases as the wave steepness S_1 increases. The wave-induced current is always smaller for 3D waves than for 2D waves, which is caused by the smaller sum-frequency effect for 3D waves than for 2D waves.
2) In a finite water depth, for both 2D and 3D nonlinear waves, the wave-induced current is larger than for linear waves, and the difference increases as the water depth decreases and as the characteristic wave steepness increases.
3) Overall, in a finite water depth, the wave-induced current for 3D waves is larger than for 2D waves for higher values of the Ursell number U_R, i.e. corresponding to relative shallow water. This is due to the smaller wave set-down effects for 3D waves than for 2D waves for higher U_R. However, for smaller values of U_R, i.e. corresponding to relative deep water, the wave-induced current for 2D waves is slightly larger than for 3D waves. This is due to the smaller wave set-down effect for both 2D and 3D waves, while the wave setup effect is larger for 2D waves than for 3D waves for relative deep water.
4) An example of results using data typical for field conditions demonstrate that the significant value of the surface Stokes drift in deep water is about 0.9% of U_{10}, which is within the range 0.8% to 1.6% of U_{10} reported by Rascle et al. (2008).

Acknowledgement

This work was carried out as part of the project "Air-Sea Interaction and Transport Mechanisms in the Ocean" funded by the Norwegian Research Council. This support is gratefully acknowledged

References

Abramowitz, M., Stegun, J.A., 1972. *Handbook of Mathematical Functions*. Dover, New York.

Bury, K.V., 1975. Statistical Models in Applied Science. John Wiley & Sons, New York

Dean, R.G., Dalrymple, R.A., 1984. *Water Wave Mechanics for Engineers and Scientists*. Prentice-Hall, Inc., New Jersey, USA.

Forristall, G.Z., 2000. Wave crest distributions: Observations and second-order theory. *J. Phys. Oceanography,* 30, 1931-1943.

Myrhaug, D., 2013. Some statistical aspects of wave-induced drift in sea states. *Coastal Eng.,* 78, 53-56.

Myrhaug, D. Stokes drift estimation based on long-term variation of wave conditions. *Proc IMechE Part M. J Engineering for the Maritime Environment,* doi: 10.1177/1475090213506699, in press.

Rascle, N., Ardhuin, F., 2013. A global wave parameter database for geophysical applications. Part 2: Model validation with improved source term parameterization. *Ocean Modelling,* 70, 174-188.

Rascle, N., Ardhuin, F., Queffeulou, P., Croizé-Fillon, D., 2008. A global wave parameter database for geophysical applications. Part 1: Wave-current-turbulence interaction parameters for the open ocean based on traditional parameterizations. *Ocean Modelling,* 25, 154-171.

Sharma, J.N., Dean, R.G., 1981. Second-order directional seas and associated wave forces. *Soc. of Petroleum Engineers Journal,* 21, 129-140.

Tucker, M.J., Pitt, E.G., 2001. *Waves in Ocean Engineering,* Elsevier, Amsterdam.

Webb, A., Fox-Kemper, B., 2011. Wave spectral moments and Stokes drift estimation. *Ocean Modelling,* 40, 273-288.

Webb, A. A., 2013. Stokes drift and meshless wave modeling. PhD Thesis, Faculty of the Graduate School, University of Colorado. http://www.geo.brown.edu/research/Fox-Kemper/pubs/pdfs/WebbThesis.pdf

Table 1. Example of results for deep water and finite water depth. The statistical quantities of the wave-induced currents u_L and M/ρ are the significant values, i.e. the expected values caused by the (1/3)rd largest wave crests.

	Deep water	Finite water depth h=15 m
$H_s(m)$	2	2
$T_p(s)$	6.7	6.7
k_p(rad/m)	0.0896	0.0993
S_1	0.029	0.029
U_R	0	0.060
$\hat{\alpha}_{2D}, \hat{\beta}_{2D}$ (Eqs. (14) and (17))	1.0484, 0.9687	1.0857, 0.9686
$\hat{\alpha}_{3D}, \hat{\beta}_{3D}$ (Eqs. (15) and (17))	1.0426, 0.9741	1.0705, 0.9746
$u_{Lrms}(z_1=0)$ (m/s) (Eq. (7))	0.0420	0.0517
$\bar{u}_{Llin}(z_1=0)$ (m/s) (Eqs. (7) and (20))	0.0881	0.108
$\bar{u}_{Lnonlin2D}(z_1=0)$ (m/s) (Eqs. (7) and (19))	0.0950	0.121
$\bar{u}_{Lnonlin3D}(z_1=0)$ (m/s) (Eqs. (7) and (19))	0.0940	0.119
M_{rms}/ρ (m^2/s) (Eq. (10))	0.234	0.260
M_{lin}/ρ (m^2/s) (Eqs. (10) and (20))	0.491	0.546
$M_{nonlin2D}/\rho$ (m^2/s) (Eqs. (10) and (19))	0.529	0.609
$M_{nonlin3D}/\rho$ (m^2/s) (Eqs. (10) and (19))	0.524	0.597
$\bar{u}_{Ldet}(z_1=0)$ (m/s)	0.0840	0.103
M_{det}/ρ (m^2/s)	0.468	0.520

Figure captions

Fig. 1 The nonlinear-to-linear ratio R_1 of the significant value of the wave-induced current according to Eq. (21) for $n = 3$ for 2D and 3D waves in deep water versus the wave steepness S_1.

Fig. 2 The ratio R_2 of the significant value of the wave-induced current for 3D waves to that for 2D waves in deep water according to Eq. (22) for $n = 3$ versus the wave steepness S_1.

Fig. 3 Isocurves for the nonlinear-to-linear ratio R_1 of the significant value of the wave-induced current according to Eq. (21) for $n = 3$ for 2D waves versus wave steepness S_1 and Ursell number U_R.

Fig. 4 Isocurves for the nonlinear-to-linear ratio R_1 of the significant value of the wave-induced current according to Eq. (21) for $n = 3$ for 3D waves versus wave steepness S_1 and Ursell number U_R.

Fig. 5 Isocurves for the ratio R_2 of the significant value of the wave-induced current for 3D waves to that of 2D waves according to Eq. (22) for $n = 3$ versus the wave steepness S_1 and Ursell number U_R.

Figure

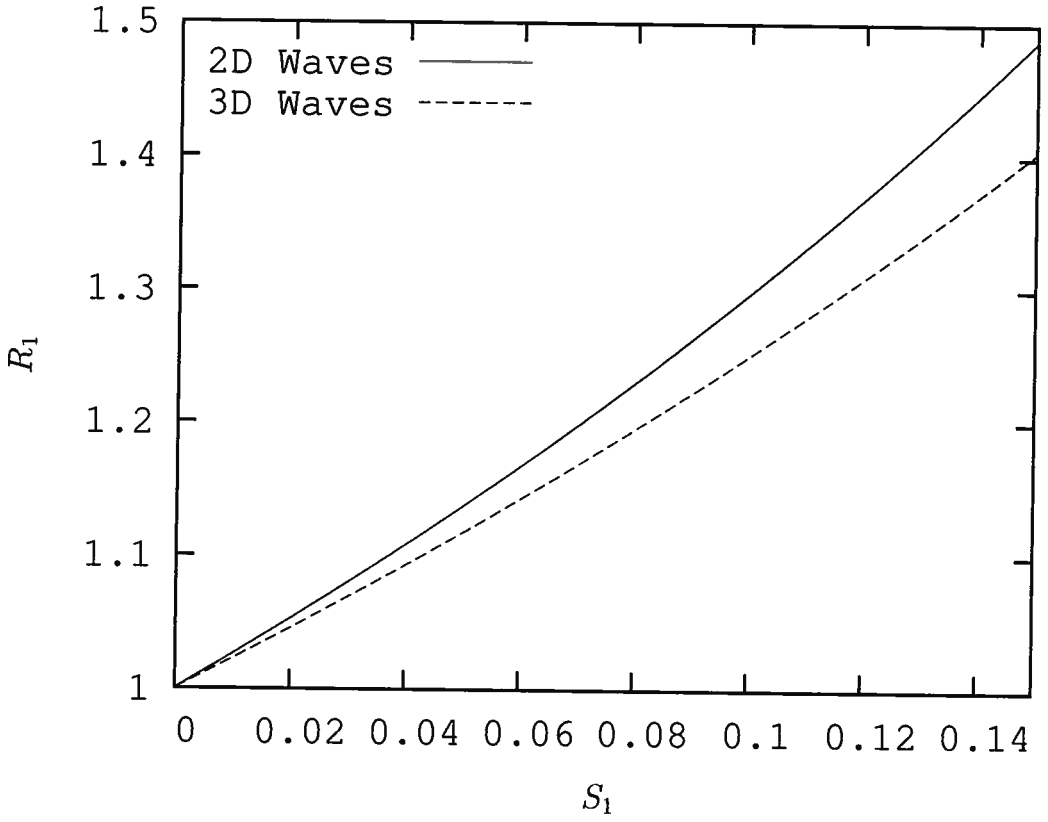

Figure 1:

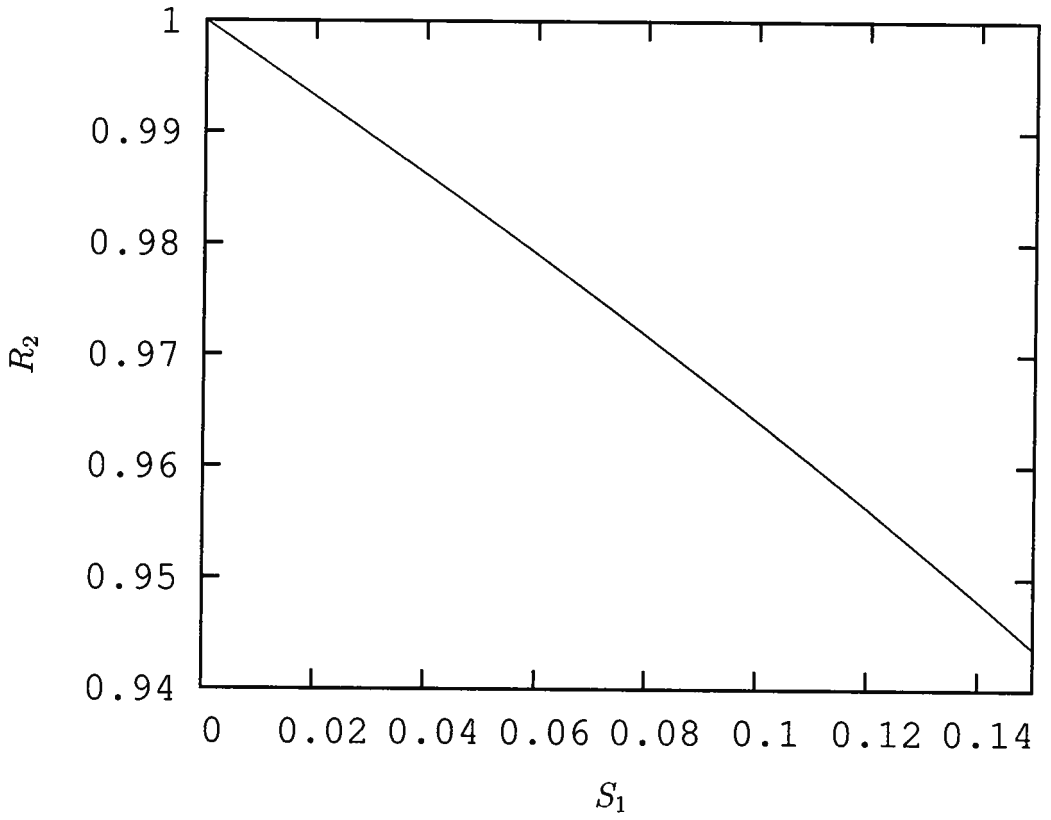

Figure 2:

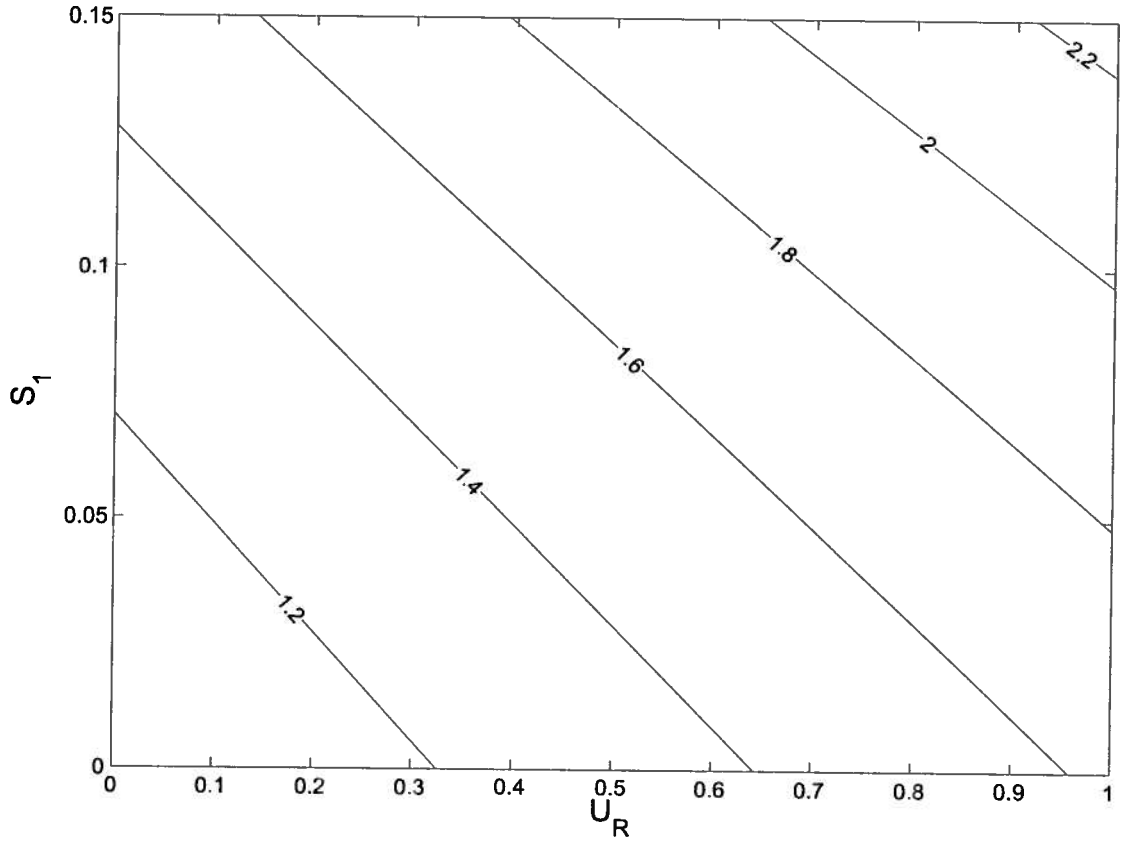

Figure 3:

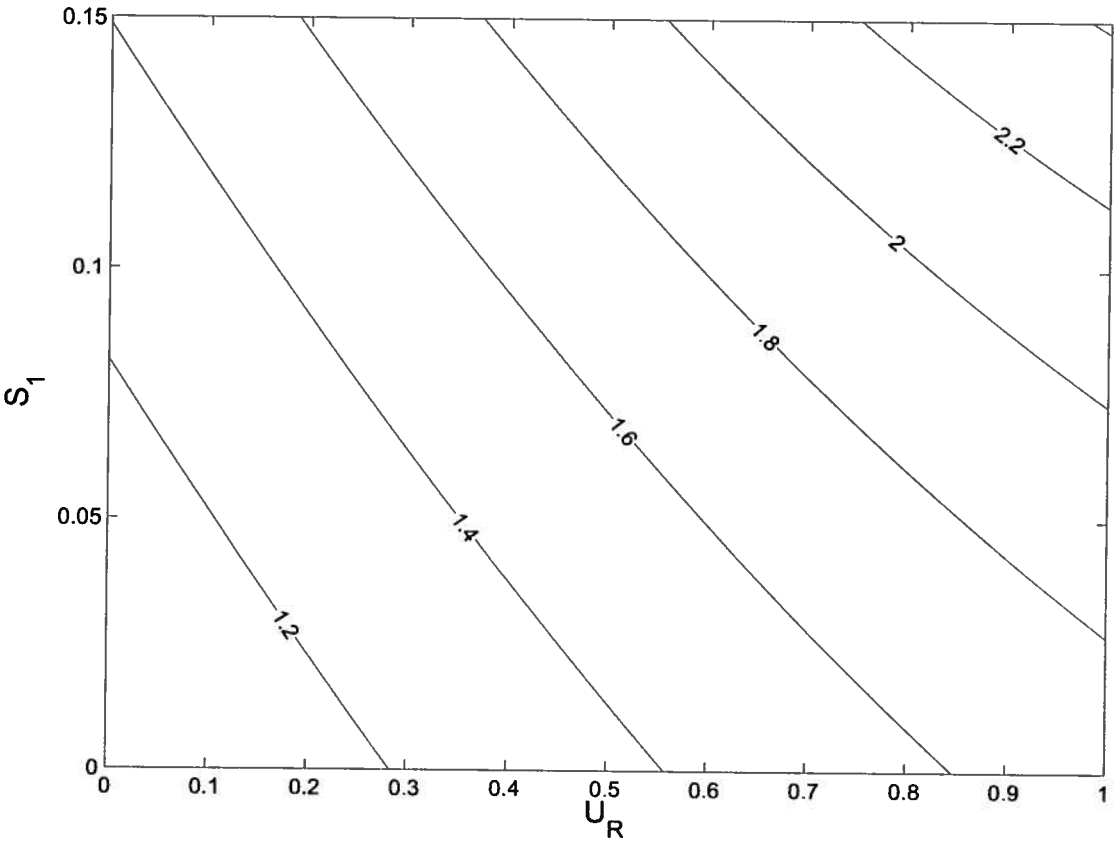

Figure 4:

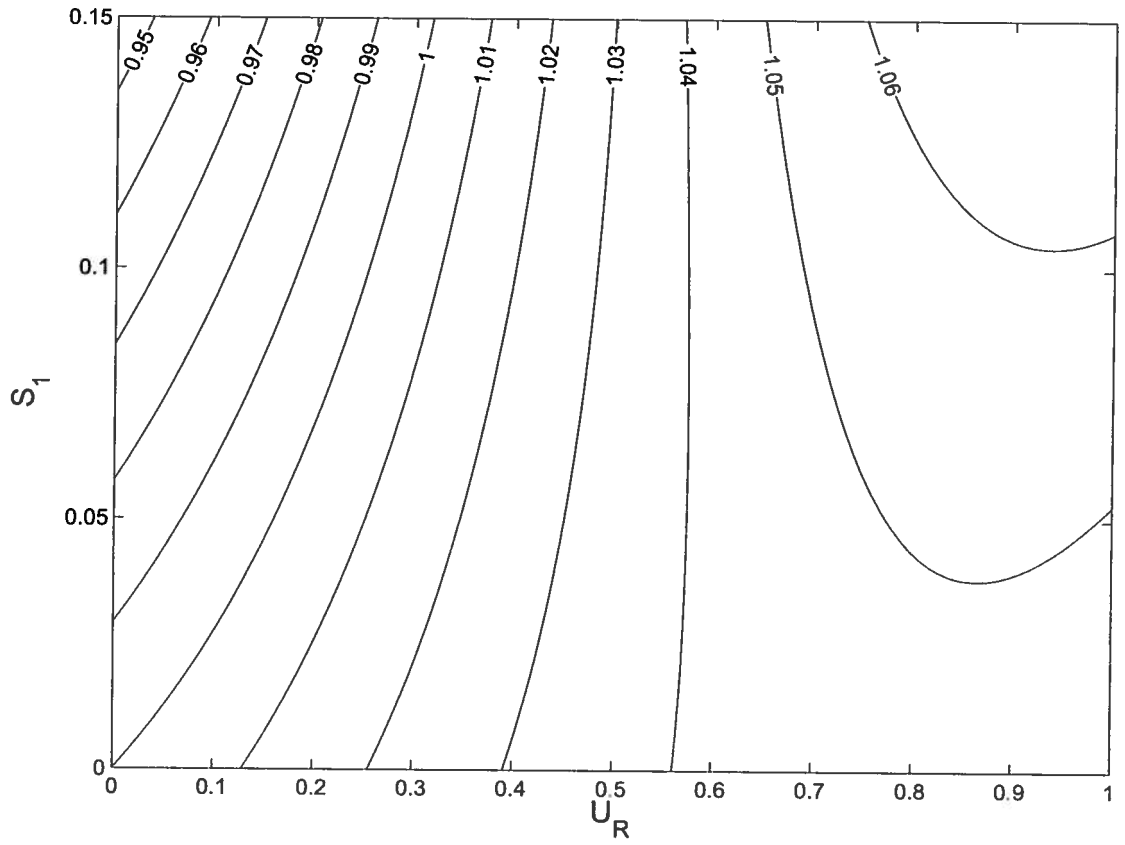
0.15
0.1
0.05
0
S_1
0.95
0.96
0.97
0.98
0.99
1
1.01
1.02
1.03
1.04
1.05
1.06
0
0.1
0.2
0.3
0.4
0.5
0.6
0.7
0.8
0.9
1
U_R

Figure 5: